

Velocity-map imaging of near-threshold photoelectrons in Ne and Ar

P. O'Keeffe,¹ P. Bolognesi,¹ R. Richter,² A. Moise,² Y. Ovcharenko,^{1,*} G. C. King,³ and L. Avaldi¹

¹*CNR Istituto di Metodologie Inorganiche e dei Plasmi, Area della Ricerca di Roma 1, Rome, Italy*

²*Sincrotrone Trieste, Area Science Park, Basovizza, Trieste, Italy*

³*School of Physics and Astronomy and Photon Science Institute, University of Manchester, Manchester, United Kingdom*

(Received 3 May 2011; published 11 August 2011)

The photoionization of Ne and Ar has been studied in the region between the $^2P_{3/2}$ and $^2P_{1/2}$ thresholds using a velocity-map imaging (VMI) spectrometer. The VMI technique provides a two-dimensional overview of the ionization cross section versus photon energy and emission angle. In these regions the neutral Rydberg states converging to the $^2P_{1/2}$ ion state affect both the ionization cross section and the asymmetry parameter of the photoelectron angular distribution, which both display Fano line shapes. The results are compared with relativistic multichannel quantum-defect calculations.

DOI: [10.1103/PhysRevA.84.025404](https://doi.org/10.1103/PhysRevA.84.025404)

PACS number(s): 32.80.Fb, 32.80.Zb

Since the early experiments in the 1930s [1], the measurement of photoelectron angular distributions (PADs) of electrons emitted in the photoionization of atoms and molecules has been a valuable tool to characterize the structure of the continuum and bound electronic states, to provide information on photoionization dynamics, and to test theoretical models. Renewed interest in these measurements has been triggered by the development of new highly efficient imaging techniques [2] and new sources [3].

Near-threshold photoionization offers the opportunity to study different aspects of photoionization. Indeed, when photoionization occurs in the region between the two spin-orbit thresholds of a rare gas, the $np^5(^2P_{1/2})ns'$ and nd' Rydberg states can be populated, and then their decay to the $^2P_{3/2}$ ion continuum affects both the cross section and the photoelectron angular distribution. While several studies of the cross section between the two spin-orbit thresholds have been reported in the literature, measurements of the PADs are scarce. This is partly due to the difficulty of measuring the PAD of electrons with kinetic energies less than 100 meV.

In the one-photon ionization of randomly oriented targets by fully linearly polarized radiation, the PAD is represented by the double differential cross section

$$\frac{d^2\sigma(E,\theta)}{dE d\Omega} = \frac{\sigma_0}{4\pi} [1 + \beta P_2(\cos \theta)], \quad (1)$$

where σ_0 is the total photoionization cross section, θ the angle of the emitted photoelectron with respect to the polarization of the radiation, $P_2(\cos \theta)$ is the second-order Legendre polynomial, and β is the asymmetry parameter. The β parameter holds information on the photoionization dynamics, because it depends on the radial matrix elements and the relative phase of the partial waves of the photoelectron in the continuum. Thus it represents a more severe test of theories than the total cross section, which depends on only the squared moduli of the ionization amplitudes [4]. The PADs of rare gases between the two spin-orbit thresholds have been studied in detail for Kr and Xe [5–9]. Measurements for Ne and Ar are

less complete. Caldwell and Krause [10] and Wu *et al.* [11] reported data in a photon energy region of about 30 meV between the two thresholds. More recently Red *et al.* [12] performed an investigation of Ne using an imaging technique. In this work we have measured the PADs for photoionization of Ne and Ar over the full energy region between the $^2P_{3/2}$ and $^2P_{1/2}$ ionic states combining the high resolution of the gas-phase beamline at Elettra and the resolution and efficiency of a recently built VMI analyzer [13].

The general layout and performance of the beamline are described elsewhere [14]. In these experiments the synchrotron radiation, which is 100% linearly polarized, is scanned over the region 15.75–15.90 and 21.56–21.66 eV in the Ar and Ne cases, respectively. The target gas was introduced into the interaction region as a continuous supersonic beam formed by expanding 1–2 bar of gas through a 50- μ m nozzle. The gas source was located at 90° with respect to the propagation direction of the synchrotron radiation, that is, along its polarization axis. A full description of the VMI apparatus as well as of the position-sensitive detector (PSD) used in these experiments and their operation modes are given in Refs. [13] and [15]. The raw images from the PSD were inverted using the PBASEX routine [16]. The method works by reconstructing the original three-dimensional (3D) distributions of the emitted electrons by fitting a set of basis functions of known inverse Abel integral to the two-dimensional (2D) projected image. We have ported the original code into a Windows-compatible program and added extensive image-processing capabilities such as the possibility to rotate the image, stretch it along one of the axes, subtract a background image, and correct by detector efficiency [17].

Photoexcitation of the p shell in a rare gas leads to two Rydberg series (ns' and nd') converging to the threshold of the excited $^2P_{1/2}$ ionic state. The higher members of these series lie in the $^2P_{3/2}$ continuum and appear as resonances in the photoionization cross section and β parameter. These series have been studied in several photoabsorption and photoionization experiments; see, for example, Refs. [18–23]. However, the small energy splitting between the two fine structure components (97 and 177.5 meV in Ne and Ar, respectively) has made the measurement of the photoelectrons difficult. Caldwell and Krause [10,11] reported measurements of the photoelectron spectra and angular distribution over a

*Present address: Institut für Optik und Atomare Physik, Technische Universität Berlin, D-10623 Berlin, Germany.

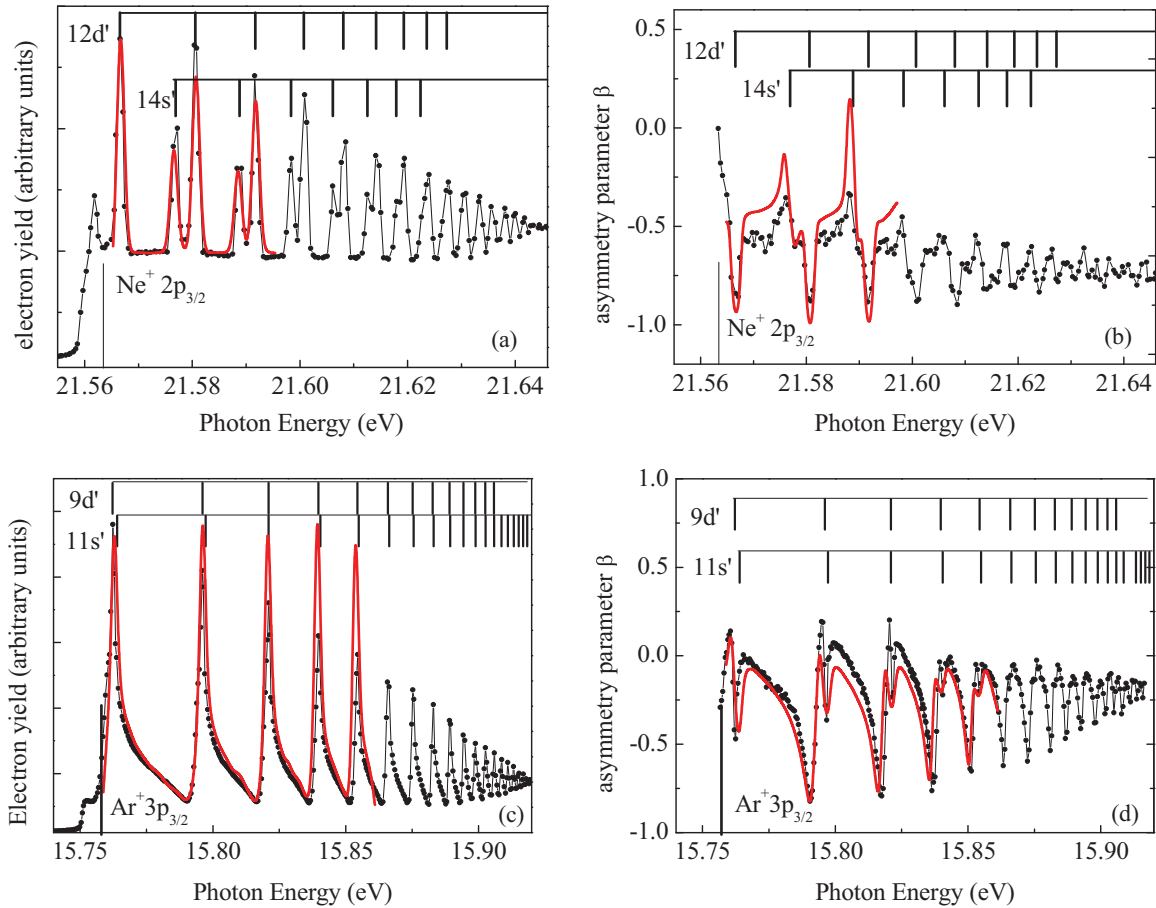


FIG. 1. (Color online) Photoelectron yield [(a) and (c)] and parameter [(b) and (d)] for the photoionization to the $\text{Ne}P^+$ [(a) and (b)] and $\text{Ar}P^+$ [(c) and (d)] $2P_{3/2}$ ionic states. The full (red) lines are the convolution of the theoretical predictions [26,27] with the Gaussian function which accounts for the experimental resolution.

region of about 30 meV, which includes the 12–14 d' and 14–15 s' resonances in Ne and the 10 d' and 12 s' resonances in Ar, while Red *et al.* [12] covered the full region in Ne using the same imaging technique as this work, but with a slightly worse overall energy resolution.

The total photoelectron yields and asymmetry parameters measured in this work are shown in Figs. 1(a)–1(d). A preliminary report of the Ne results has been presented in Ref. [24]. At each photon energy, a velocity-mapped photoelectron image was acquired for 180 s. Each image was then background subtracted and inverted using the software described above in order to extract the β parameter for each photon energy, while the total electron yield was derived simultaneously from the integral of counts in the image. The overall energy resolution is determined by the $\Delta E/E$ of the VMI spectrometer, where E is the kinetic energy of the photoelectrons and amounts to a few percent [13]. The typical relative uncertainty on the measured β parameter is ± 0.02 when comparing adjacent photon energy points, while the overall absolute uncertainty due to possible systematic errors related to background subtraction is estimated to be of the order of ± 0.05 .

The energy resolution and efficiency of the experimental setup allow the ns' and nd' Rydberg series of Ne to be distinguished up to the 18 s' and 17 d' members [Fig. 1(a)].

In the case of the Ar spectrum [Fig. 1(c)], the sharp peaks of the ns' series overlap and dominate the broad features due to the $(n-2)d'$ series. Here Rydberg states with n as high as 26 are observed. The nonvanishing photoelectron yield below the $^2P_{3/2}$ threshold is produced by field ionization due to the electrostatic field in the interaction region of the VMI apparatus.

Ne and Ar photoionization in the region between the two spin orbit thresholds was studied theoretically by Johnson and Le Dourneuf [25] and Johnson *et al.* [26] within the framework of relativistic multichannel quantum-defect theory (MQDT). The parameters for the MQDT analysis were obtained from an *ab initio* relativistic random-phase approximation calculation. Radojević and Talman [27] extended the calculations in the case of Ne to include seven *jj*-coupled channels in order to take into account the interaction of the $2p$ shell with the adjacent $2s$ shell. The present Ne results are compared with the predictions by Radojević and Talman [27] and those of Ar with the calculations of Johnson *et al.* [26]. In the latter case the data in the energy region of the lowest five resonances have been extracted from Fig. 4 of Ref. [26]. For the comparison the theoretical predictions have been convoluted with a Gaussian function to take into account the experimental energy resolution. In Ne a good agreement is found between the observed and the predicted energy positions of the resonances, while a slight shift is observed

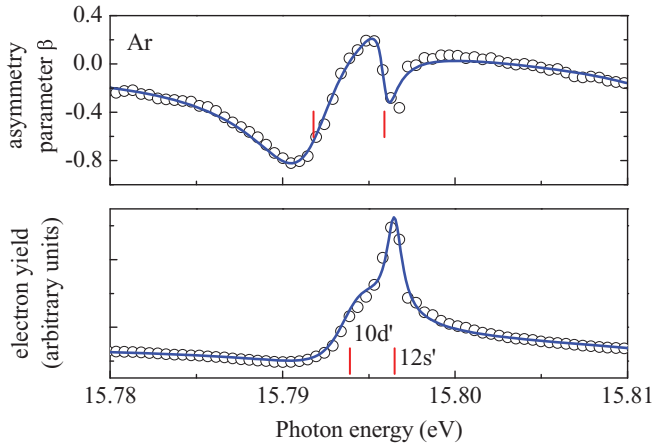


FIG. 2. (Color online) Total electron yield (bottom panel) and β parameter (top panel) in the region of the $12s'$ and $10d'$ autoionizing states in Ar. The full line is the best fit to the experimental data using Eq. (2); see text. The corresponding parameters are reported in Table I.

in Ar. This is consistent with the findings of Ref. [18], where theory was compared with a photoabsorption spectrum. The shape of the resonances does not change along the series in the experimental spectrum. This is in agreement with the calculated weak energy dependence of the quantum-defect parameters. This weak dependence of the quantum-defect parameters results also in an almost constant value of the predicted cross sections for the different resonances [26]. In contrast, in both the present and photoabsorption measurements [18], a rapid decrease of the peak intensities is observed in the ns' and nd' series. This is mainly an instrumental effect due to the finite experimental resolution. Indeed an unperturbed Rydberg series is characterized by an oscillator strength and a linewidth which both decrease as $(1/n^*)^3$, where n^* is the effective quantum number. Therefore, when the resolution is much narrower than the natural linewidth, the peaks will have a constant height, with a width that decreases as $(1/n^*)^3$. When the instrumental resolution is not negligible with respect to the natural linewidth, then the peak height is not constant and the integrated areas show a $(1/n^*)^3$ dependence [28]. Fluorescence decay to lower lying neutral states, as observed for example in the case of the He doubly excited states [29], might also contribute to the observed trend in the peak intensities. In the case of Ne, theory [27] predicts a width for the ns' series that is about five times larger than that of the nd' series. However, the very small values of

these widths (for example, 62 and 13 μeV for the $14s'$ and $12d'$ states [27]) prevent this difference being observed in the present measurements.

The photon energy dependencies of the β parameters are shown in Figs. 1(b) and 1(d). The autoionizing resonances produce sharp variations superimposed on a β value, which monotonically approaches values of about -0.7 and -0.1 near the $^2P_{1/2}$ ionic threshold in the cases of Ne and Ar, respectively. In Ne the ns' resonances result in β values that are less negative while the opposite occurs at the nd' peaks. The general trend is consistent with the measurements by Southworth *et al.* [30], who observed a minimum value of -0.6 at about 22.5 eV and a rise toward threshold. Caldwell and Krause [10] quoted a value of -0.17 ± 0.15 in the region between the $13d'$ and $15s'$ resonances, which is greater than the average value measured in the present work. The same occurs for the β values measured in Ref. [12], which are always larger than -0.4 . In the Ar case, the general behavior of β is consistent with the sparse measurements near threshold taken by Wannberg *et al.* [31]. The strongly negative value (-0.55) measured by those authors at 93 meV above the $^2P_{3/2}$ state is clearly explained by the combined effect of the $13d'$ and $15s'$ Rydberg states on the shape of β in that region. The values measured by Wu *et al.* [11] between 15.79 and 15.82 eV agree with the present ones within the respective experimental uncertainties. The experimental β parameters have been compared also with theoretical values calculated in Refs. [27] and [26] for Ne and Ar, respectively. For this comparison the theoretical calculations have been convoluted with the experimental resolution according to the procedure given in [27] using the same Gaussian function adopted in the convolution of the photoelectron yield. A good agreement as for the observed shape and the absolute values is obtained in Ar, while in Ne theory appears to overestimate the rise in the β value near the ns' Rydberg states.

In the Ar case the nd' and ns' series are more clearly identifiable in the β parameter measurement than in the photoelectron yield, because the features due to autoionization appear at different energy positions and are broader than those in the photoelectron yield. This is clearly shown in Fig. 2 for the region of the Ar $10d'$ and $12s'$ states. Recently Grum-Grzhimailo *et al.* [32] have shown that all the observables or vector correlation parameters of the photoionization process (i.e., the anisotropy coefficient of the angular distribution of the photoelectrons, the spin polarization of the photoelectrons, the alignment and orientation of the photoion) display a Fano-like behavior in the region of an autoionizing peak. Moreover the width and energy shift of these features with respect to the same features in the photoionization spectrum follow a

TABLE I. The q and ρ^2 resonance profile parameters of the $12s'$ and $10d'$ autoionizing states in Ar obtained by the measured shift (Δ) and broadening (χ) of the features in the asymmetry parameter compared with experimental and theoretical literature data. In the last column, the experimental widths used in the derivation of the resonance profile parameters are listed.

	Present work				Ref. [21]		Semiempirical MQDT [34] ^a		RRPA-MQDT [26] ^a		Ref. [22] $\Gamma(\text{meV})$
	Δ (meV)	χ	q	ρ^2	q	ρ^2	q	ρ^2	q	ρ^2	
$10d'$	-1.7 ± 0.5	1.3 ± 0.6	2.1 ± 0.4	0.45 ± 0.05	2.06 ± 0.2	0.48 ± 0.05	2.52	0.49	1.86	0.57	3.8 ± 0.12
$12s'$	-0.5 ± 1.0	4.25 ± 1.9	19.4 ± 5	0.8 ± 0.5	16.5 ± 6.8	0.08 ± 0.06	10.86	0.15	10.86	0.11	0.065 ± 0.006

^aExtracted from Figs. 8–10 of Ref. [21]

universal scaling law. This has been shown in a fluorescence polarimetry experiment on the Xe $4d^{-1}5/26p$ ($J=1$) resonance by the same authors [32] and by Tauro and Liu [33] in the case of the photoelectron angular distributions of the two-photon excited autoionizing I atoms formed in the photolysis of CH₃I. Thus we have fitted two Fano lineshapes, labeled 1 and 2 for the $10d'$ and $12s'$ states, respectively, in Eq. (2), to the experimental data:

$$T = \sigma_a^T + \sigma_{b_1}^T (q_1 + \tilde{\epsilon}_1)^2 / (1 + \tilde{\epsilon}_1^2) + \sigma_{b_2}^T (q_2 + \tilde{\epsilon}_2)^2 / (1 + \tilde{\epsilon}_2^2), \quad (2)$$

where T is either the ionization cross section or the β parameter in the measurements of the angular distribution; the q 's are the asymmetry profile parameters; and σ_a and σ_b are the interacting and noninteracting parts of the cross section in the case of photoelectron yield measurements and specific quantities in the case of the profiles in the vector correlation parameters [32], $\epsilon = (E - E_r) / (\Gamma/2)$, where E is the photon energy and E_r and Γ are the energy and width of the autoionizing state. The energy \tilde{E}_r and width $\tilde{\Gamma}$ of the feature in the vector correlation parameter are related to those measured in the photoionization spectrum by the relationships [32]

$$\tilde{E}_r = E_r + \Delta; \quad \tilde{\Gamma} = \chi \Gamma. \quad (3)$$

In the Ar case, the β parameters show negative shifts $\Delta = -1.7 \pm 0.5$ meV and -0.5 ± 0.5 meV and broadening factors $\chi = 1.3$ and 4.25 for the $10d'$ and $12s'$ autoionizing states, respectively. By using these values and the natural widths of the states [22], one can derive values for q_i and $\rho_i^2 = \sigma_{b_i} / (\sigma_{b_i} + \sigma_a)$ of the autoionizing state using Eqs. (12) and (13) of [32]. In Table I the present values are compared with the experimental and theoretical values of Ref. [21] as well as with those calculated from the semiempirical MQDT parameters of Lee and Lu [34] and from *ab initio* Relativistic Random Phase Approximation, RRP A, MQDT calculations [26]. A good agreement is observed in the case of the $10d'$ state for both the q and ρ^2 parameters. For the $12s'$ state the determined value of q is in agreement within the experimental uncertainty with the experimental value of Ref. [21], but larger than the theoretical ones. The ρ^2 value obtained in this work is definitely larger than previous experimental and theoretical values. This is due to the finite-energy resolution of the measurements. Indeed, working back from the measured q and ρ^2 values of Ref. [21] with Eq. (13) of [32], the expected value of the energy shift is about 0.04 meV. This is a value that is out of reach with present-day photoelectron techniques at synchrotron sources.

In conclusion, the use of the VMI technique has allowed the total photoionization spectrum and the angular distribution of the photoelectrons in the near-threshold region to be

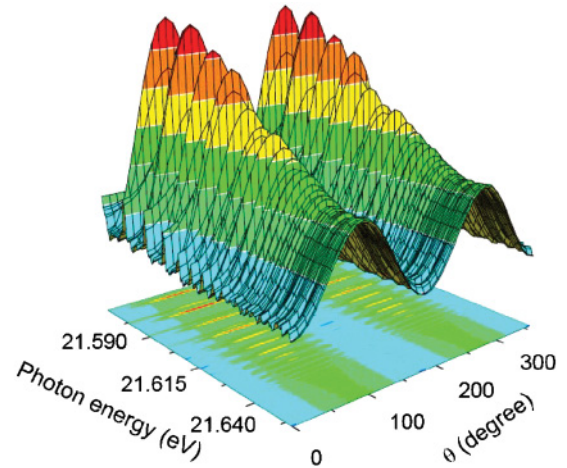


FIG. 3. (Color online) Surface and contour plots of the photoelectron yield vs photon energy and emission angle for the photoionization of Ne⁺ $2P_{3/2}$ ionic state.

measured simultaneously, thus providing a two-dimensional overview of the partial ionization cross section versus photon energy and emission angle, as shown in Fig. 3 for Ne. Up to now a two-dimensional (2D) overview of the photoionization cross section has only been achieved using the magnetic angle-changing technique [35,36], but only for kinetic energies above 100 meV or using conventional photoelectron spectroscopy in very limited energy ranges [10,11]. Moreover, it should be noted that the VMI technique allows both photoelectron spectra and PADs to be recorded near the threshold, while other threshold techniques, such as threshold photoelectron spectroscopy (TPES) [37], provide spectra of higher energy resolution but without any angular resolution.

The analysis of a subset of the present Ar data, on one hand, has confirmed the properties of the vector correlation parameters, which can be used to extract the resonance profile parameters. On the other hand, this analysis has shown the limit of the application of this approach in the case of measurements where photoelectrons are detected with a finite-energy resolution that is not negligible with respect to the natural width of the state.

This research was partly supported by the FP7 Marie Curie Reintegration Grant 230980 and the Elettra Long-Term Project 2008096. Y. Ovcharenko acknowledges the Elettra-ICTP Program for supporting his participation in the measurements.

- [1] E. O. Lawrence and M. A. Chaffee, *Phys. Rev.* **36**, 1099 (1930).
 [2] A. T. J. B. Eppink and D. H. Parker, *Rev. Sci. Instrum.* **68**, 3477 (1997).
 [3] F. J. Wuilleumier and M. Meyer, *J. Phys. B: At. Mol. Opt. Phys.* **39**, R425 (2006).
 [4] C. M. Lee, *Phys. Rev. A* **10**, 1598 (1974).

- [5] Y. Morioka *et al.*, *J. Phys. B: At. Mol. Opt. Phys.* **18**, 71 (1985).
 [6] T. A. Carlson *et al.*, *J. Chem. Phys.* **89**, 1464 (1988).
 [7] J. A. R. Samson and J. L. Gardner, *Phys. Rev. Lett.* **31**, 1327 (1973).
 [8] M. Spieweck, M. Drescher, F. Gierschner, R. Irrgang, and U. Heinzmann, *Phys. Rev. A* **58**, 1589 (1998).

- [9] D. R. Cooper *et al.*, *J. Electron Spectrosc. Rel. Phenom.* **112**, 129 (2000).
- [10] D. Caldwell and M. O. Krause, *J. Phys. B: At. Mol. Opt. Phys.* **23**, 2233 (1990).
- [11] J. Z. Wu *et al.*, *Phys. Rev. A* **42**, 1350 (1990).
- [12] E. C. Red *et al.*, *Rev. Mex. Fis.* **S56**, 100 (2010).
- [13] P. O’Keeffe *et al.*, *Rev. Sci. Instrum.* **82**, 033109 (2011).
- [14] R. R. Blyth *et al.*, *J. Electron Spectrosc. Relat. Phenom.* **101–103**, 959 (1999).
- [15] G. Cautero *et al.*, *Nucl. Instrum. Methods Phys. Res. A* **595**, 447 (2008).
- [16] G. A. Garcia, L. Nahon, and I. Powis, *Rev. Sci. Instrum.* **75**, 4989 (2004).
- [17] Program available from the authors on request.
- [18] K. Radler and J. Berkowitz, *J. Chem. Phys.* **70**, 216 (1979).
- [19] M. A. Baing and J. P. Connerade, *J. Phys. B: At. Mol. Phys.* **17**, 1785 (1984).
- [20] K. Ito *et al.*, *J. Opt. Soc. Am. B* **5**, 2006 (1988).
- [21] K. Maeda, K. Ueda, and K. Ito, *J. Phys. B: At. Mol. Opt. Phys.* **26**, 1541 (1993).
- [22] U. Hollestein, H. Palm, and F. Merkt, *Rev. Sci. Instrum.* **71**, 4023 (2000).
- [23] D. Klar *et al.*, *Z. Phys. D: At. Mol. Clusters* **23**, 101 (1992).
- [24] P. O’Keeffe *et al.*, *J. Phys. Conf. Ser.* **288**, 012020 (2011).
- [25] W. R. Johnson and M. Le Dourneuf, *J. Phys. B: At. Mol. Opt. Phys.* **13**, L13 (1980).
- [26] W. R. Johnson, K. T. Cheng, K.-N. Huang, and M. Le Dourneuf, *Phys. Rev. A* **22**, 989 (1980).
- [27] V. Radoiević and J. D. Talman, *J. Phys. B: At. Mol. Opt. Phys.* **23**, 2241 (1990).
- [28] P. M. Dehmer, P. J. Miller, and W. A. Chupka, *J. Chem. Phys.* **80**, 1030 (1984).
- [29] J. E. Rubensson *et al.*, *Phys. Rev. Lett.* **83**, 947 (1999).
- [30] S. H. Soutworth *et al.*, *Nucl. Instr. Meth. A* **246**, 782 (1986).
- [31] B. Wannberg *et al.*, *J. Phys. B: At. Mol. Opt. Phys.* **19**, 2267 (1986).
- [32] A. N. Grum-Grzhimailo *et al.*, *J. Phys. B: At. Mol. Opt. Phys.* **38**, 2545 (2005).
- [33] S. Tauro and K. Liu, *J. Phys. B: At. Mol. Opt. Phys.* **41**, 225001 (2008).
- [34] C. M. Lee and K. T. Lu, *Phys. Rev. A* **8**, 1241 (1973).
- [35] F. H. Read and J. M. Channing, *Rev. Sci. Instrum.* **67**, 2372 (1996).
- [36] M. Zubek *et al.*, *J. Phys. B: At. Mol. Opt. Phys.* **29**, L239 (1996).
- [37] R. I. Hall *et al.*, *Meas. Sci. Technol.* **3**, 316 (1992).